Electronic Supplementary Material (ESI) for Journal of Materials Chemistry A.

Ni_2FeS_4 as highly efficient earth-abundant co-catalyst in photocatalytic hydrogen evolution

Supplementary Information

J. Zander, R. Marschall

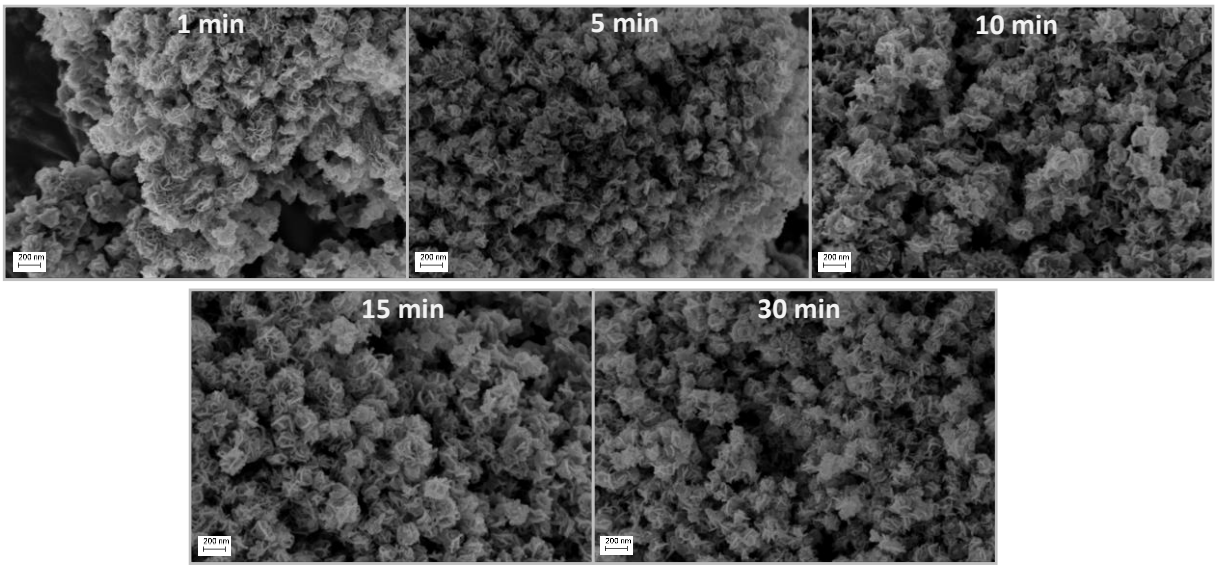

Figure S1 SEM images of Ni_2FeS_4 obtained after different synthesis durations.

Table S1 Element composition as determined *via* EDX (green) and XPS (blue). Values are average for several point areas for EDX.

EDX; XPS	1 min	5 min	10 min	15 min	30 min
At.% O	41.73 ± 5.42 40.69	21.00 ± 2.11	35.25 ± 5.59	34.53 ± 0.51 35.54	32.05 ± 2.21 38.40
At.% Ni	14.80 ± 2.51 7.10	5.80 ± 1.57	12.10 ± 5.80	17.08 ± 0.05 5.92	16.83 ± 0.46 7.15
At.% Fe	7.50 ± 1.85 2.99	2.63 ± 0.72	6.05 ± 3.18	8.83 ± 0.17 3.0	8.70 ± 0.52 3.83
At.% S	27.27 ± 10.89 17.80	12.20 ± 8.00	20.15 ± 10.11	29.65 ± 0.21 18.16	30.53 ± 1.35 24.70
At.% C	16.30 ± 7.62 31.41	61.90 ± 6.42	26.40 ± 24.75	9.88 ± 0.38 37.37	11.78 ± 0.26 25.92
Ni:Fe	2.04 ± 0.49 2.37	2.21 ± 0.16	2.03 ± 0.11	1.92 ± 0.03 1.97	1.94 ± 0.10 1.87
M:S	0.92 ± 0.39 0.567	0.81 ± 0.29	0.90 ± 0.01	0.87 ± 0.002 0.491	0.84 ± 0.02 0.444
SO_4^{2-}/S^{2-}	1.07			0.96	1.13

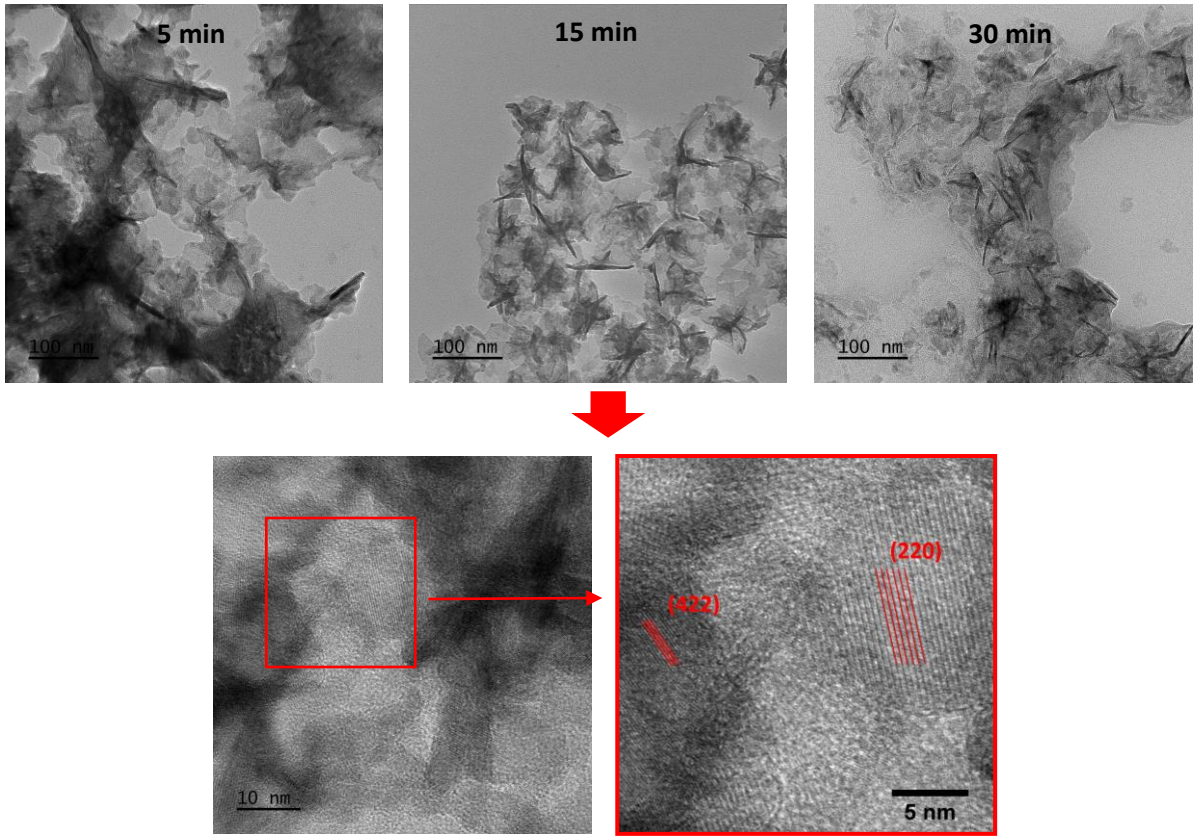

Figure S2 TEM images of Ni_2FeS_4 synthesised for different times in the microwave, including lattice planes corresponding to the (422) and (220) planes in the samples synthesised for 15 min.

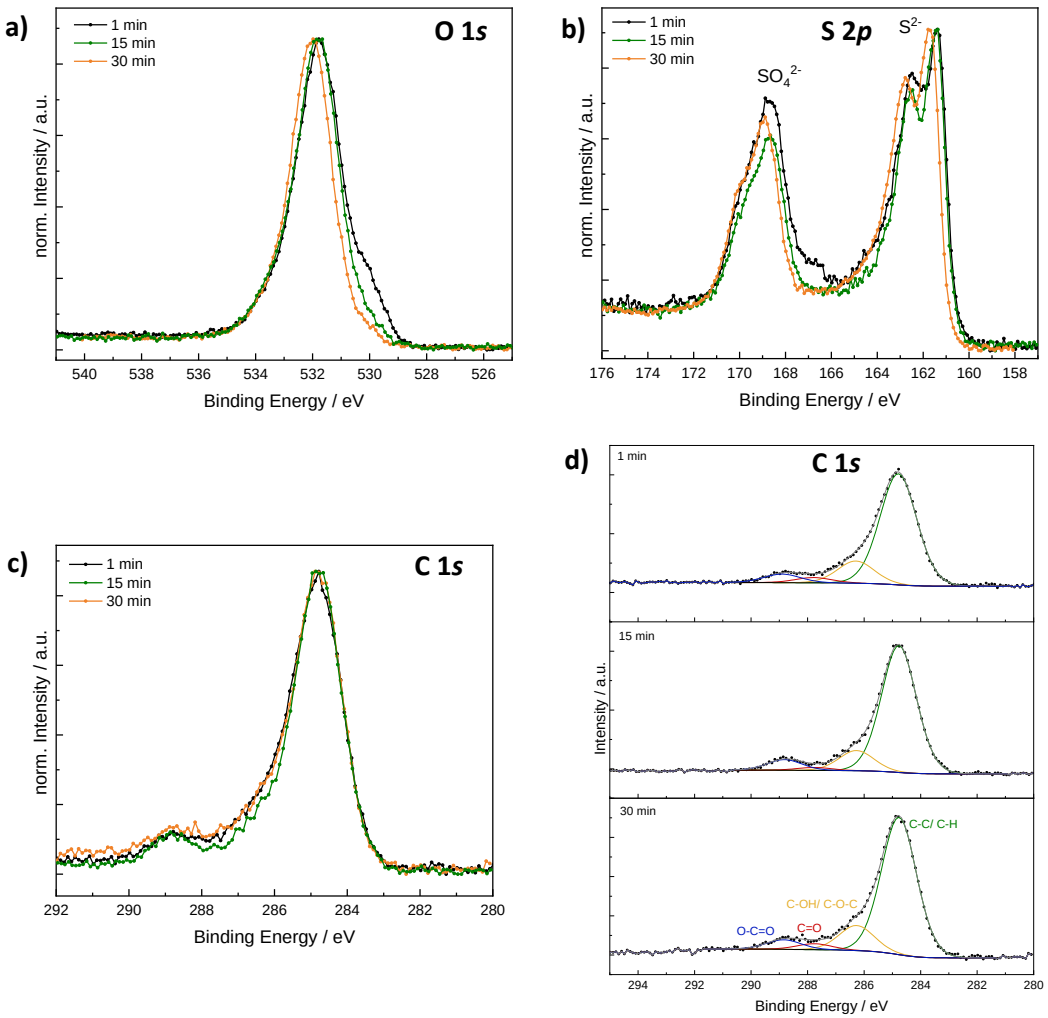

Figure S3 Normalised O 1*s* spectra (a), S 2*p* spectra (b) and C 1*s* spectra (c), as well as fitted C 1*s* spectra (d) for Ni_2FeS_4 synthesised for 1, 15 and 30 min.

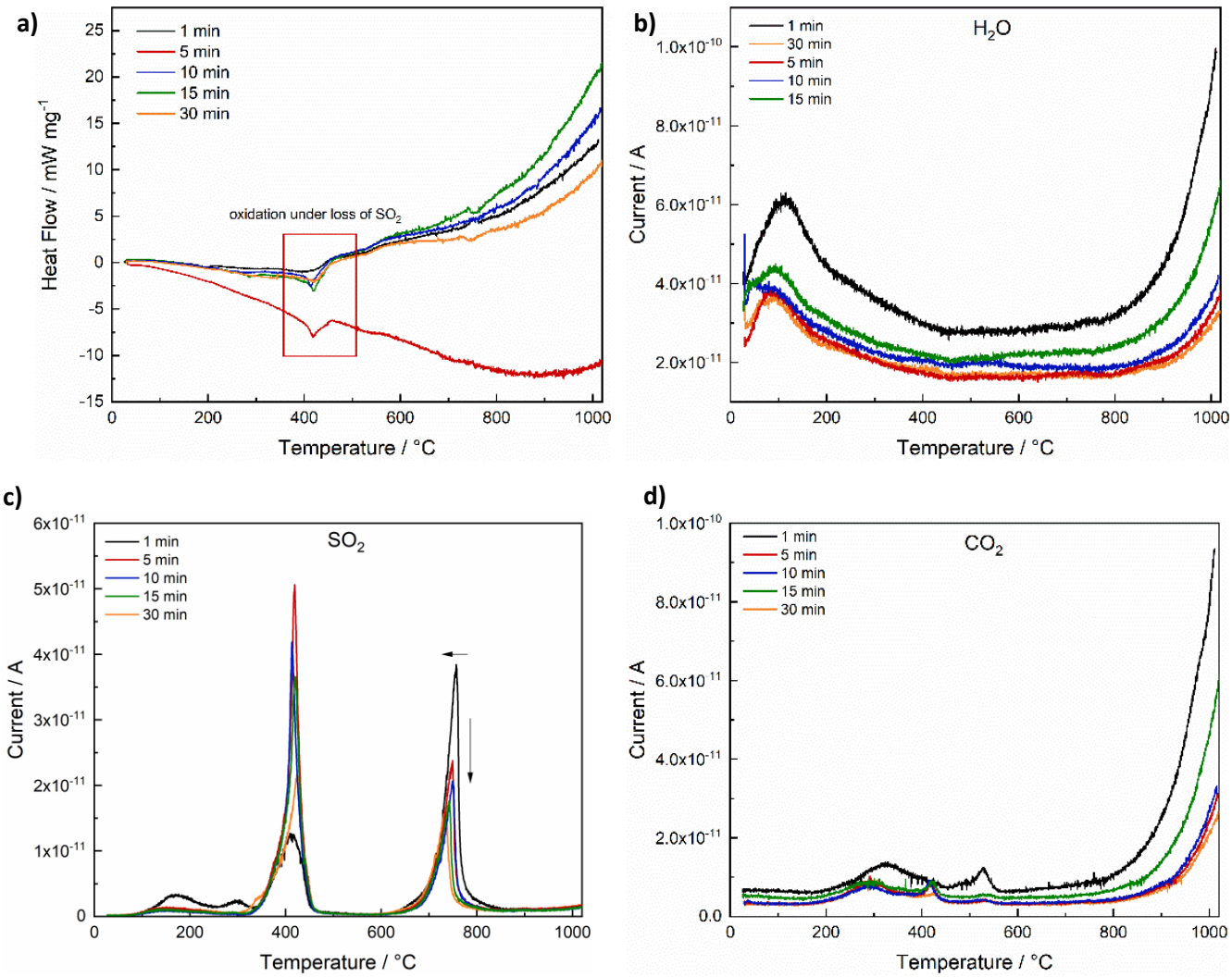

Table S2 SO_2 peak areas and relative ratios.

Synthesis Time	Area SO_2-1 [A/°C/mg]	Area SO_2-2 [A/°C/mg]	Sum [A/°C/mg]	SO_2-1/ SO_2-2
1 min	$3.04 \cdot 10^{-10}$	$6.00 \cdot 10^{-10}$	$9.03 \cdot 10^{-10}$	0.51
5 min	$5.77 \cdot 10^{-10}$	$3.61 \cdot 10^{-10}$	$9.38 \cdot 10^{-10}$	1.60
10 min	$5.66 \cdot 10^{-10}$	$3.74 \cdot 10^{-10}$	$9.40 \cdot 10^{-10}$	1.51
15 min	$7.99 \cdot 10^{-10}$	$4.66 \cdot 10^{-10}$	$1.26 \cdot 10^{-10}$	1.71
30 min	$4.48 \cdot 10^{-10}$	$3.33 \cdot 10^{-10}$	$7.81 \cdot 10^{-10}$	1.34

Figure S4 TG-MS measurements for Ni_2FeS_4 with different synthesis durations. DSC curves during a heating with 2 K/min (a) and corresponding gas evolutions monitored with MS: H_2O evolution (b), SO_2 evolution (c), and CO_2 evolution (d).

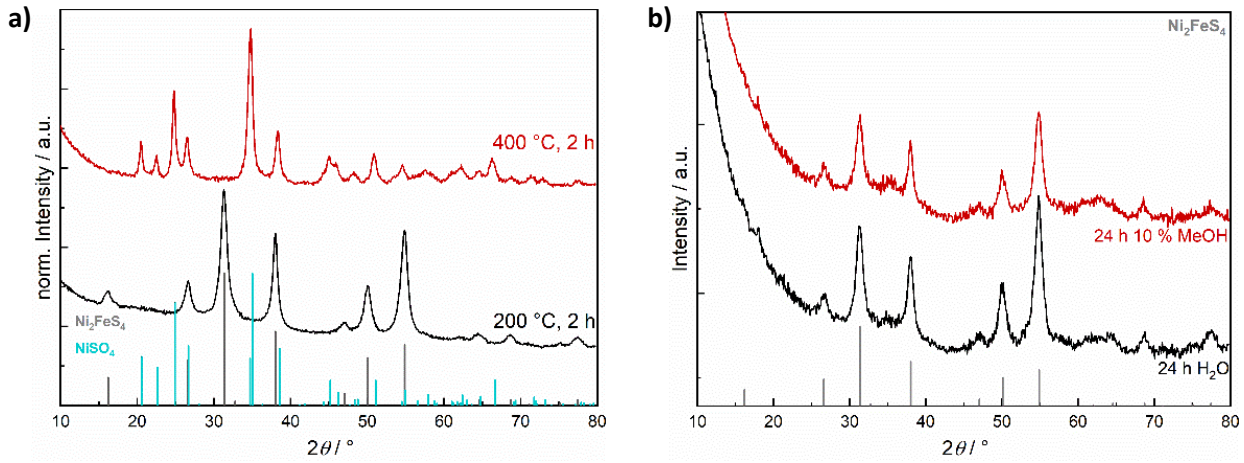

Figure S5 XRD patterns after post-synthetic heat treatment of Ni_2FeS_4 (30 min synthesis time) for 2 h at 200 and 400 °C (a) and after dispersion in H_2O/ 10 vol.% aqueous methanol (b).

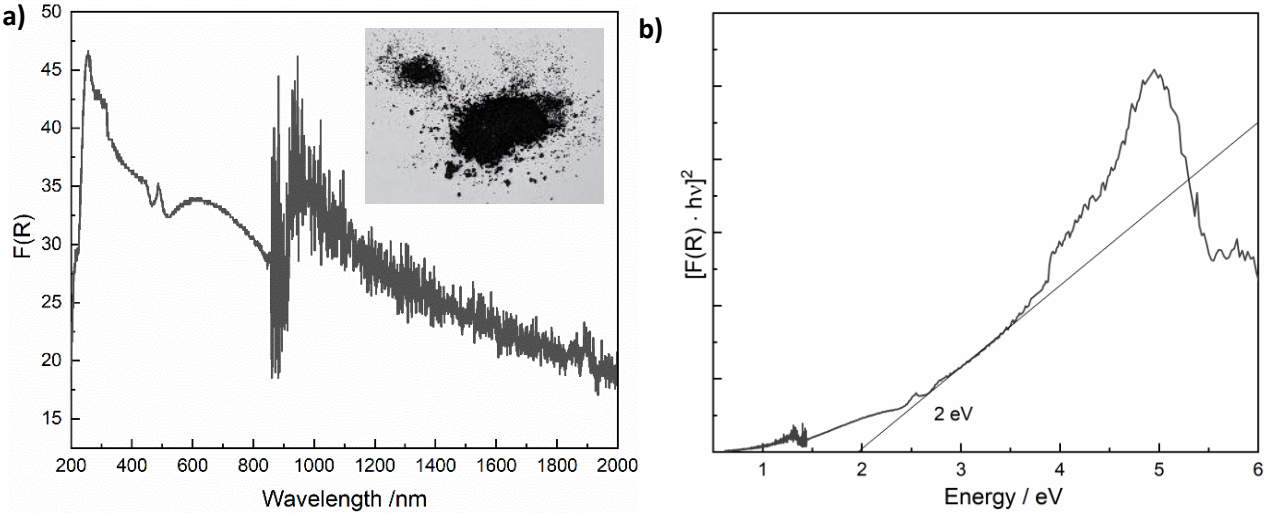

Figure S6 Kubelka-Munk (a) and direct Tauc plot (b) for Ni_2FeS_4 obtained after 30 min at 200 °C, elucidating the strong light absorption properties of the sulphide well into the NIR region.

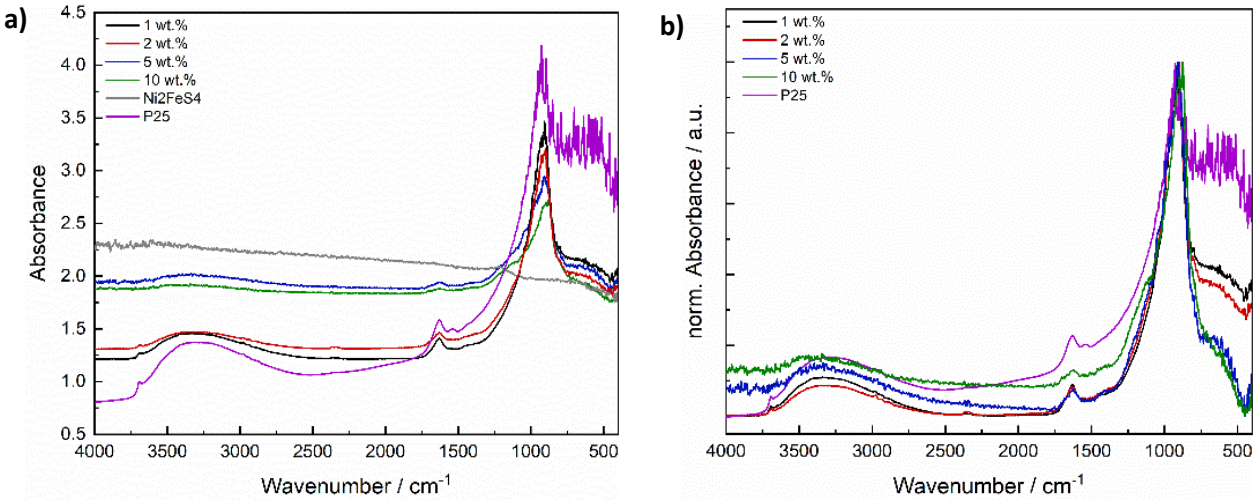

Figure S7 DRIFT spectra for P25 after loading with different amounts of Ni_2FeS_4 without normalisation (a) and normalised (b), to better show the offset caused by the absorption of Ni_2FeS_4.

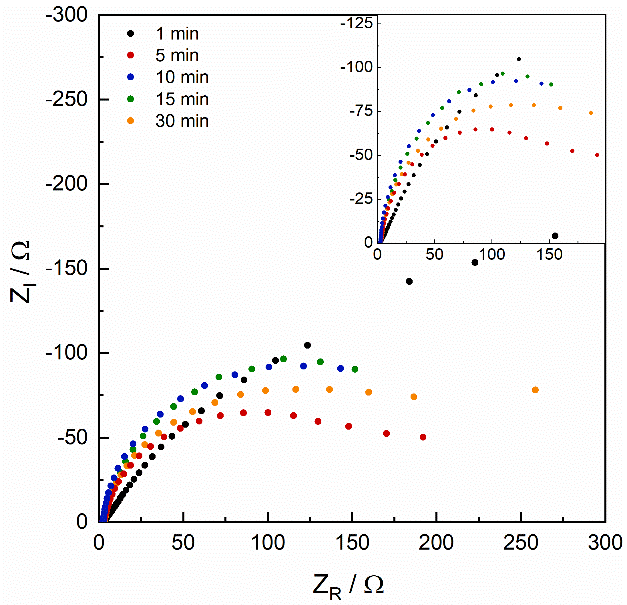

Figure S8 Nyquist plots for Ni_2FeS_4 obtained after different synthesis durations. The impedance measurements were conducted on carbon fibre electrodes in 1 M KOH at open circuit potential.

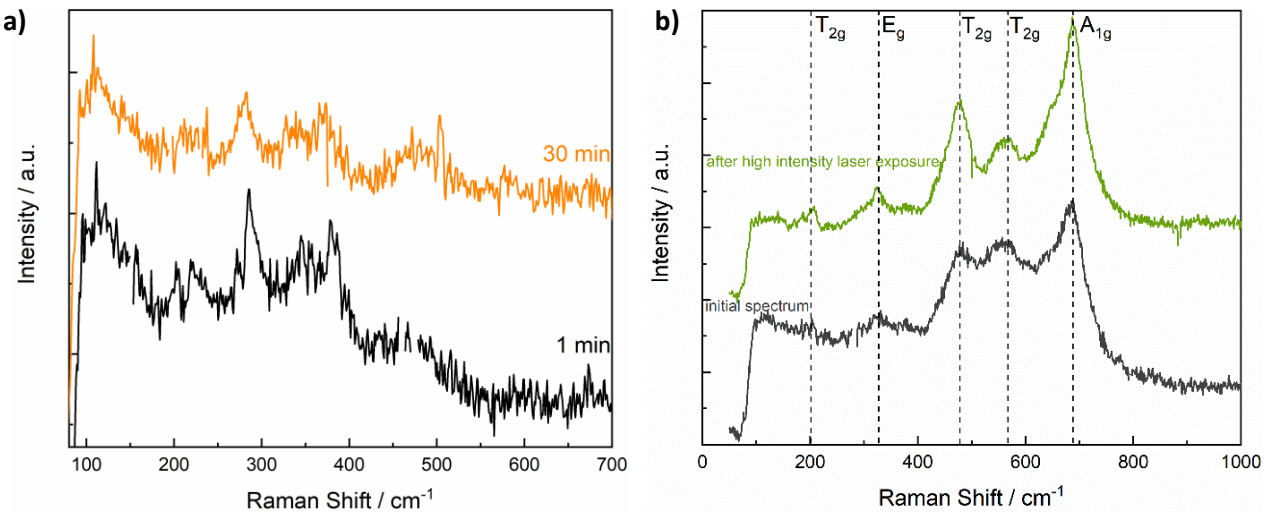

Figure S9 Raman spectra for Ni_2FeS_4 obtained after 1 and after 30 min at low laser intensity are shown in (a) and the transformation to a typical inverse spinel structure, most probably $NiFe_2O_4$, is shown in (b) first at lower laser power but already enough for oxidation (black) and then at a higher laser power (green).

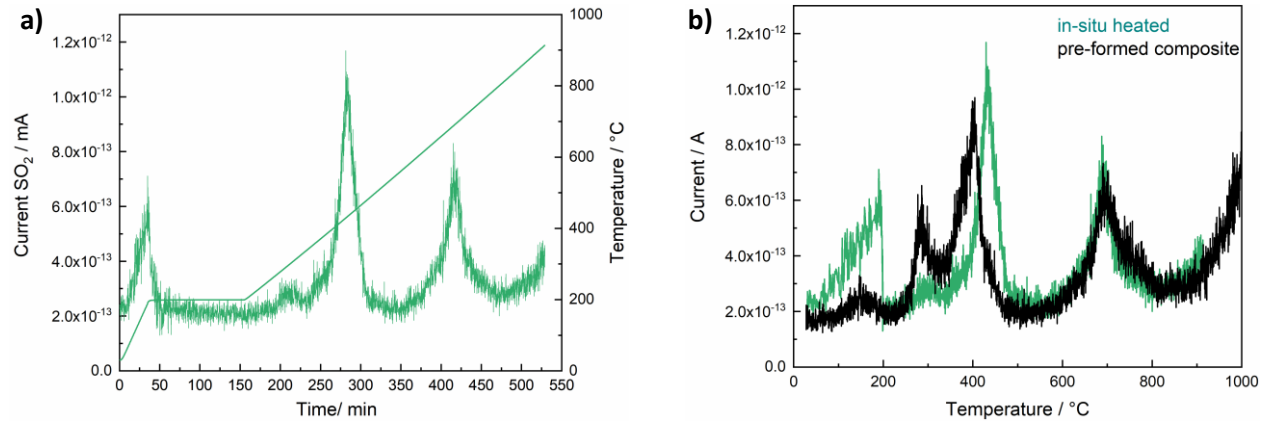

Figure S10 SO_2 gas evolution and temperature profile over time for TiO_2 and Ni_2FeS_4 ground together, but not annealed prior to the TG-MS measurement (a) and MS response for m/z=64 (SO_2) depending on the temperature for a pre-formed and an in-situ formed composite of TiO_2 and 5 wt.% of Ni_2FeS_4 (b).

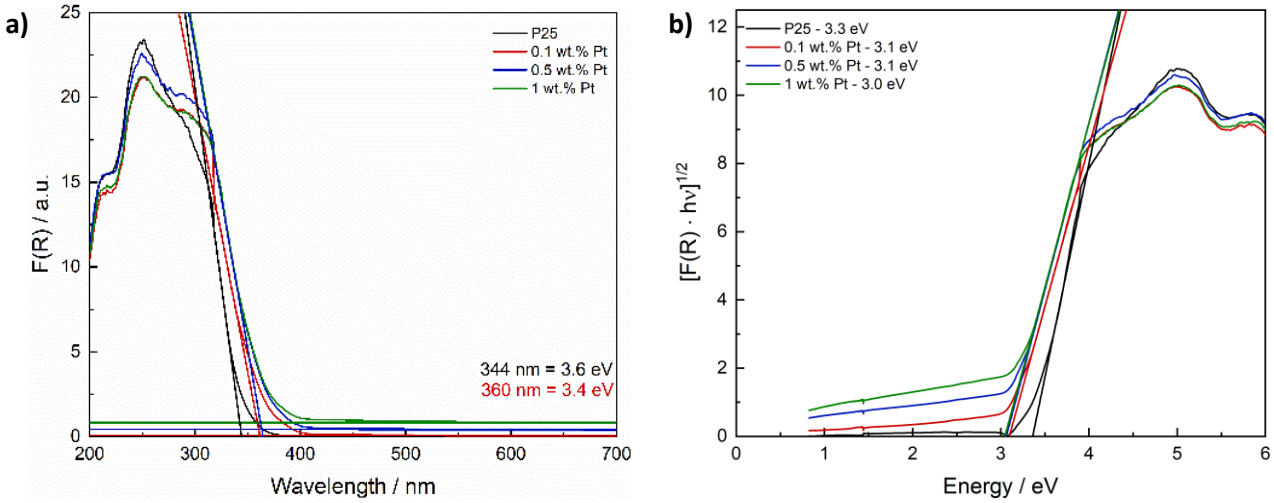

Figure S11 Kubelka-Munk (a) and indirect Tauc plot (b) of P25 before and after photo-deposition of Pt.

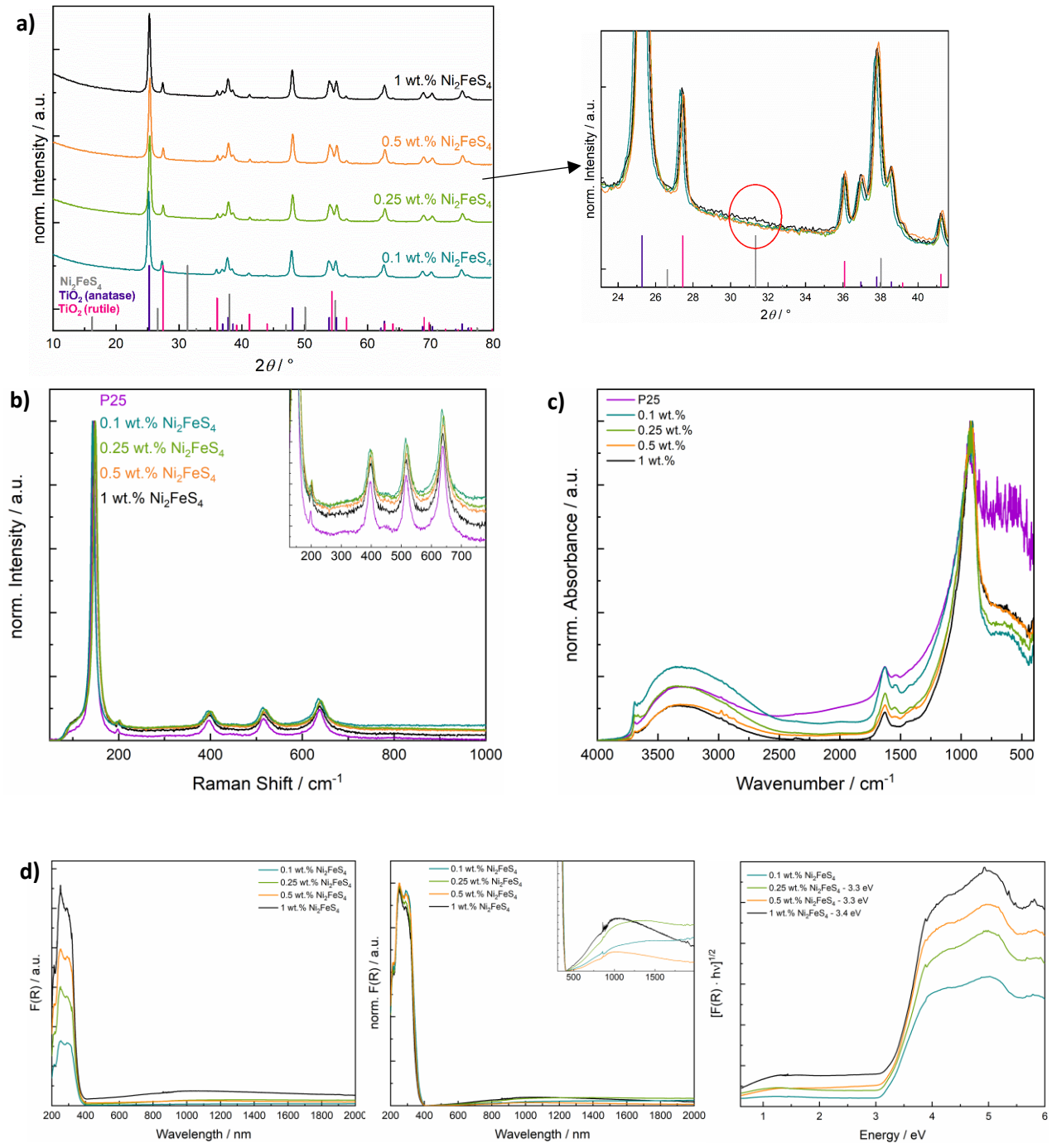

Figure S12 Cu-XRD patterns for TiO_2 loaded with Ni_2FeS_4 including 0.1 wt.% and 0.5 wt.% (a), corresponding Raman spectra (b), DRIFT spectra (c) and UV/vis/NIR spectra (d). At low loadings with Ni_2FeS_4, an increased pseudo-absorption in the UV region is additionally visible.

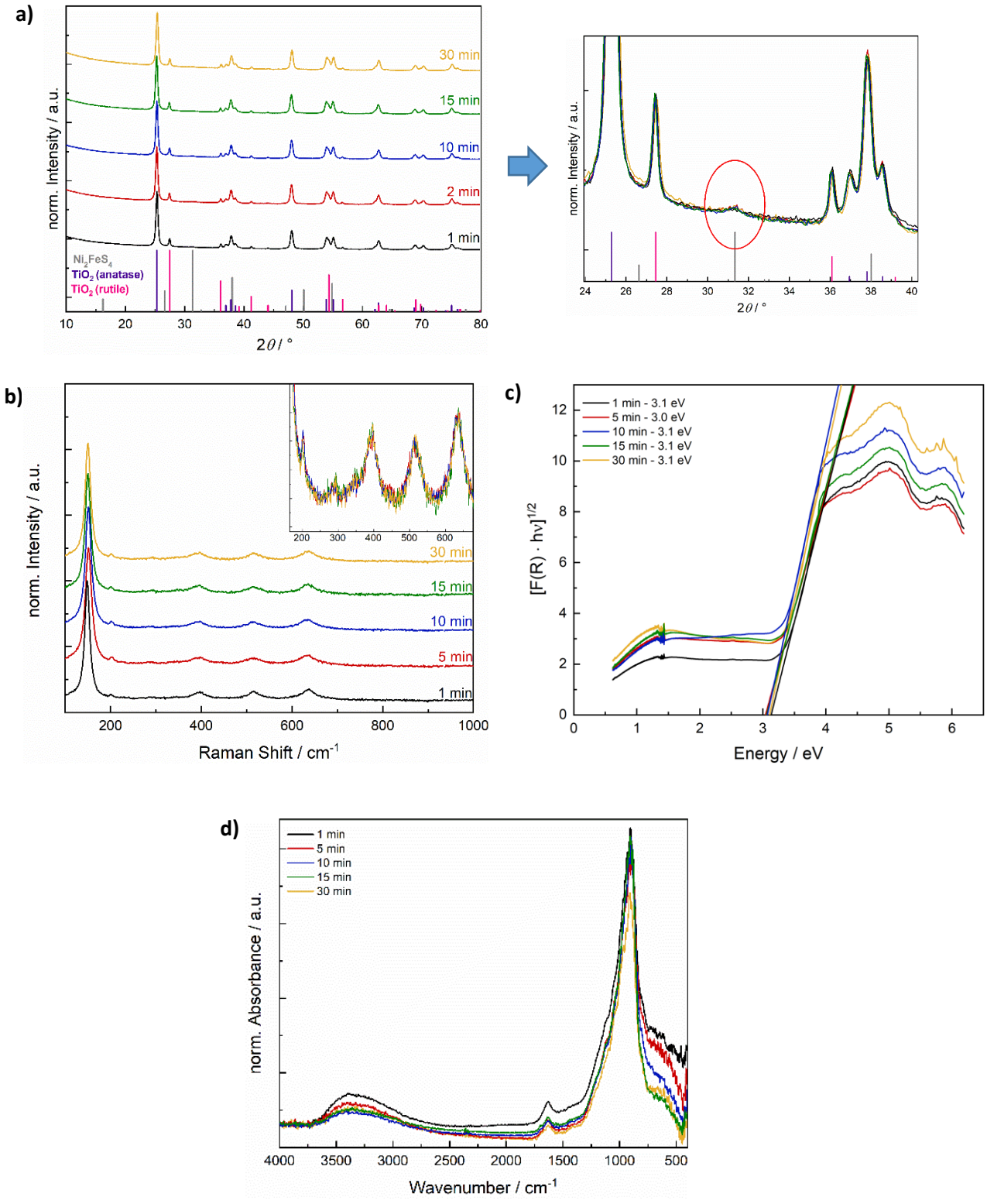

Figure S13 XRD patterns of Ni_2FeS_4 obtained after different synthesis times and loaded on TiO_2 in 5 wt.% (a), corresponding Raman spectra (b), UV/vis/NIR spectra (c) and DRIFT spectra (d).

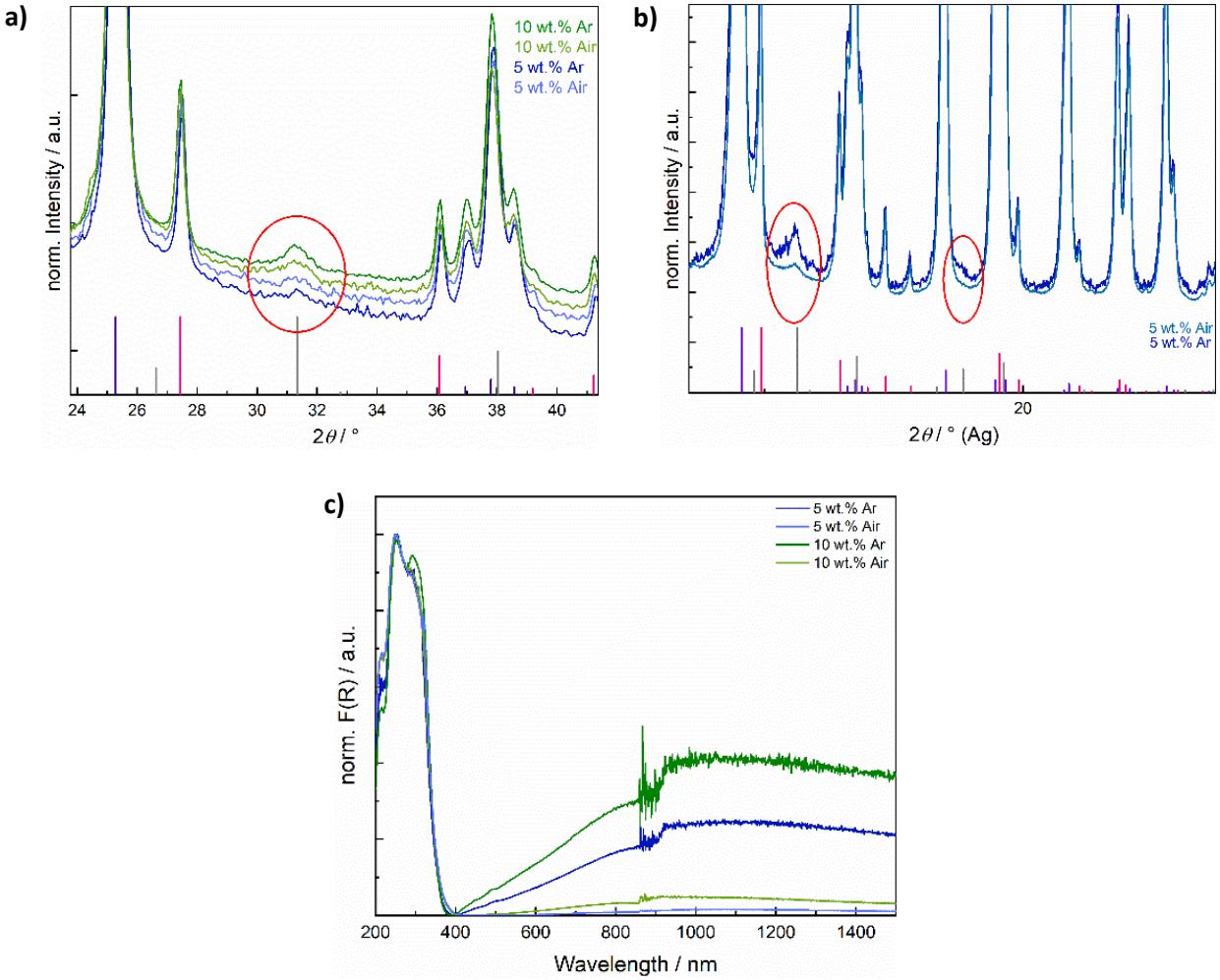

Figure S14 Comparative XRD patterns for a loading of 5 and 10 wt.% at TiO_2 and calcination in Ar *vs.* in air – Cu radiation (a), Ag radiation (b) and corresponding UV/vis/NIR spectra (c).

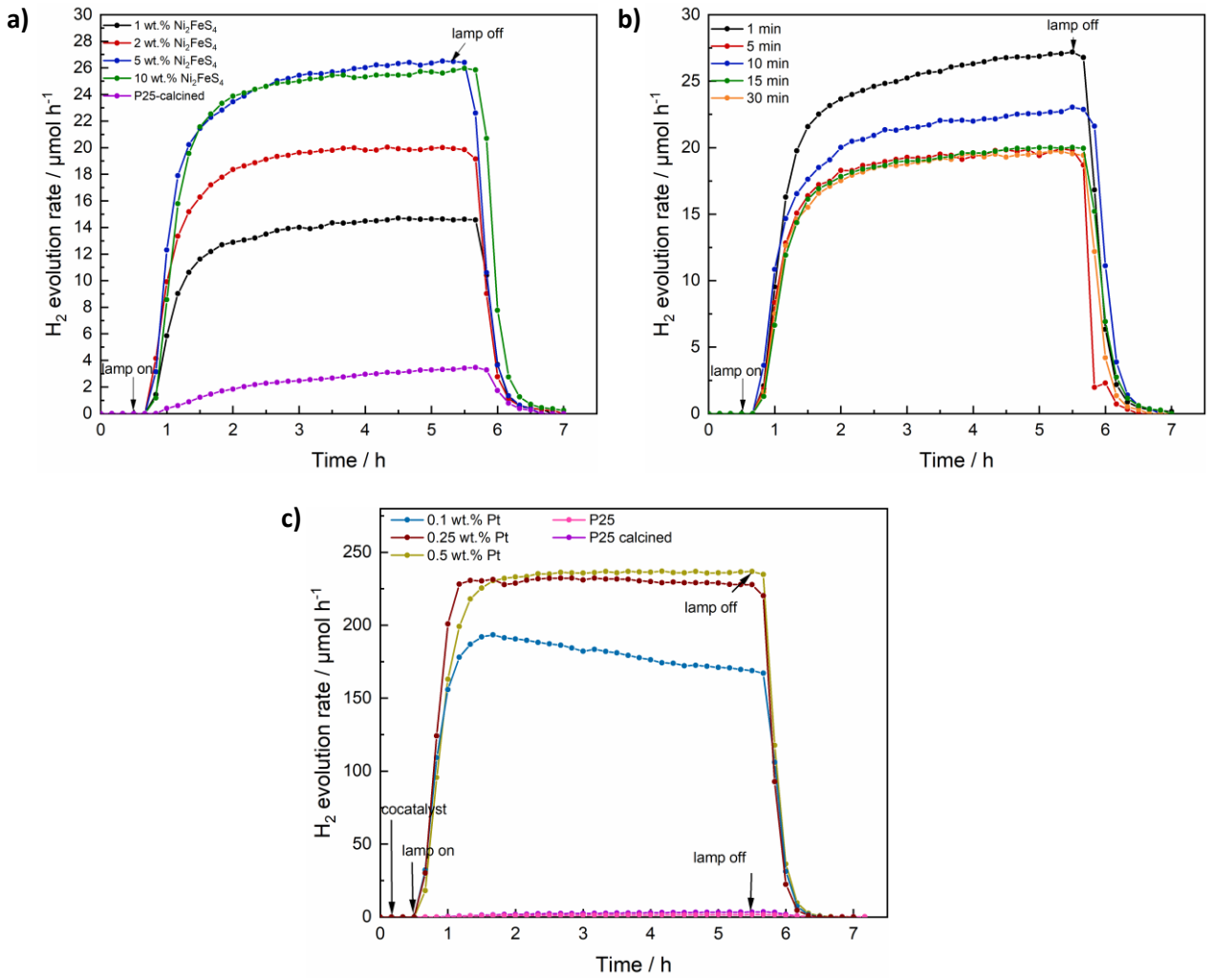

Figure S15 Hydrogen evolution for Ni_2FeS_4 on TiO_2 with different loadings and annealing in air (a) and for 5 wt.% of Ni_2FeS_4 (annealed in air) synthesised for different durations (b). Comparative measurements using photodeposited Pt as cocatalyst (d).

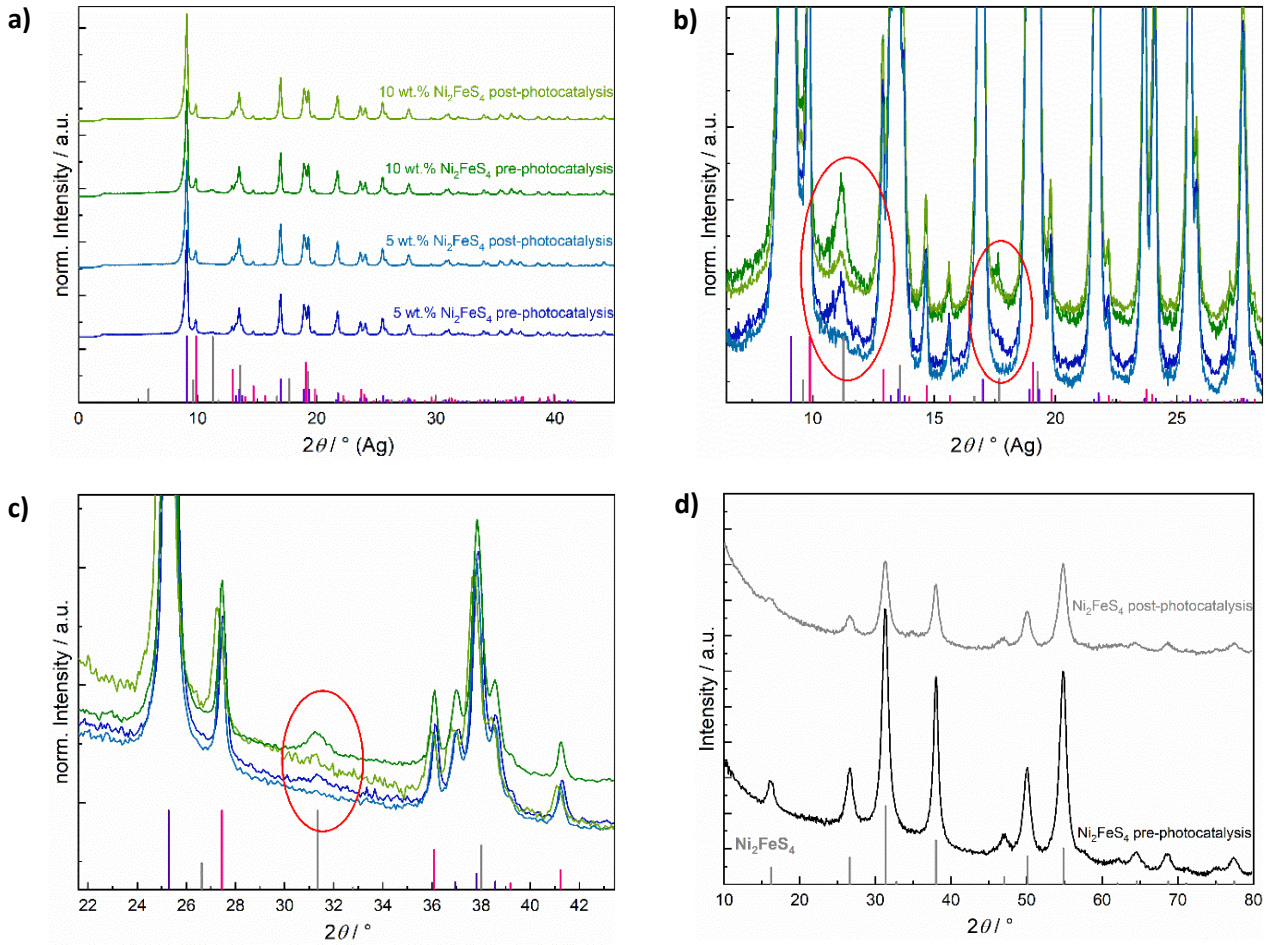

Figure S16 Ag-XRD patterns for 5 and 10 wt.% loading at TiO_2 before and after photocatalysis (a and b), Cu-XRD patterns of the same samples (c) and of Ni_2FeS_4 before and after photocatalysis with a Hg lamp(d).

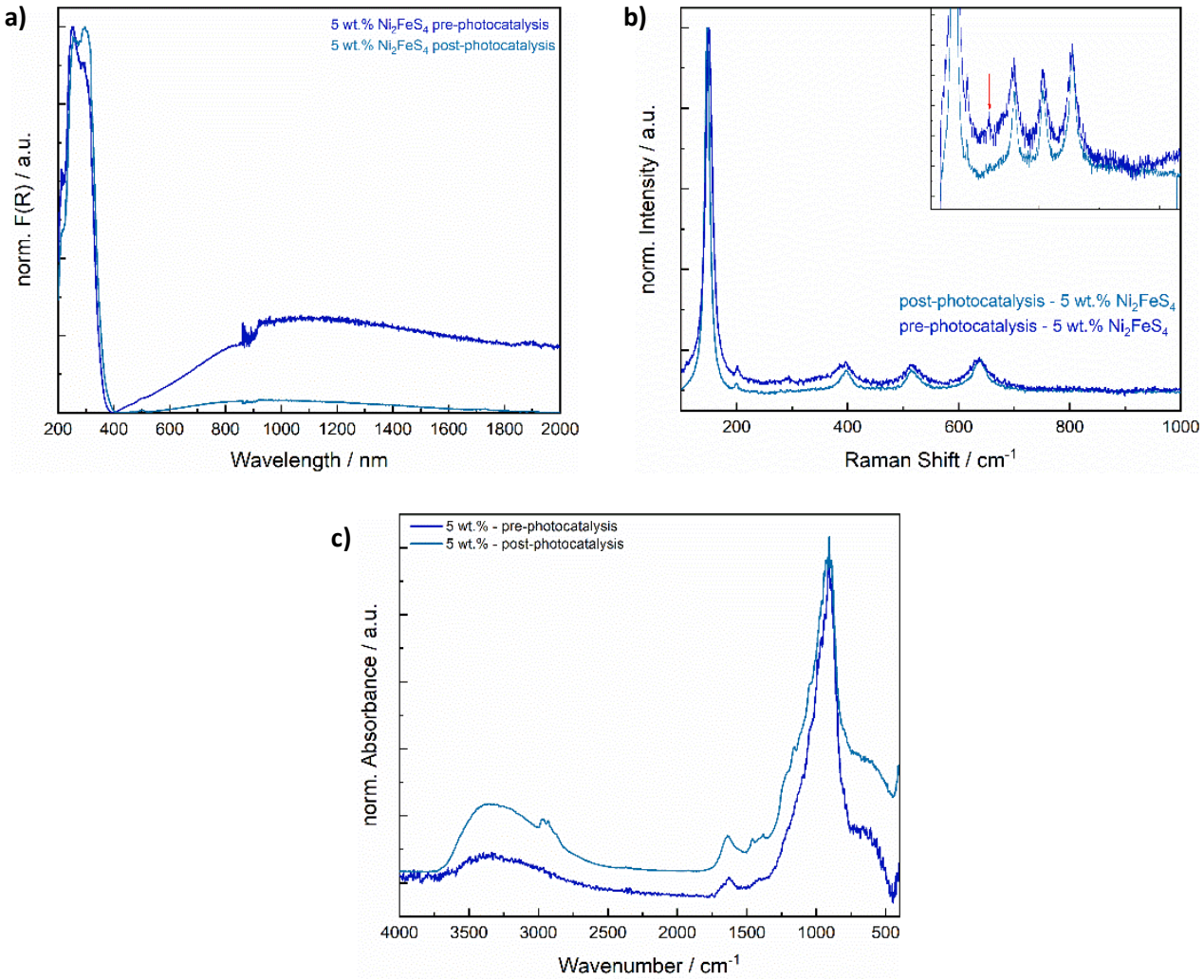

Figure S17 Comparison of TiO_2 loaded with 5 wt.% of Ni_2FeS_4 before and after photocatalysis: UV/vis/NIR spectra (a), Raman spectra (b) and DRIFT spectra (c).

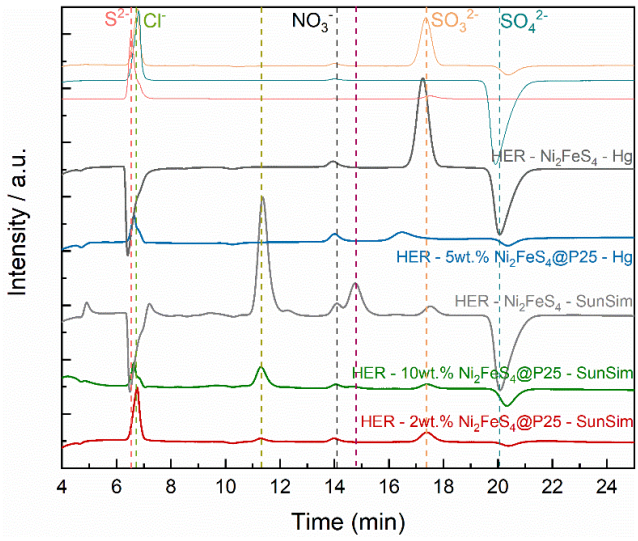

Figure S18 Ion-Chromatography for selected samples after the photocatalysis, showing the evolution of SO_3^{2-} and SO_4^{2-}.

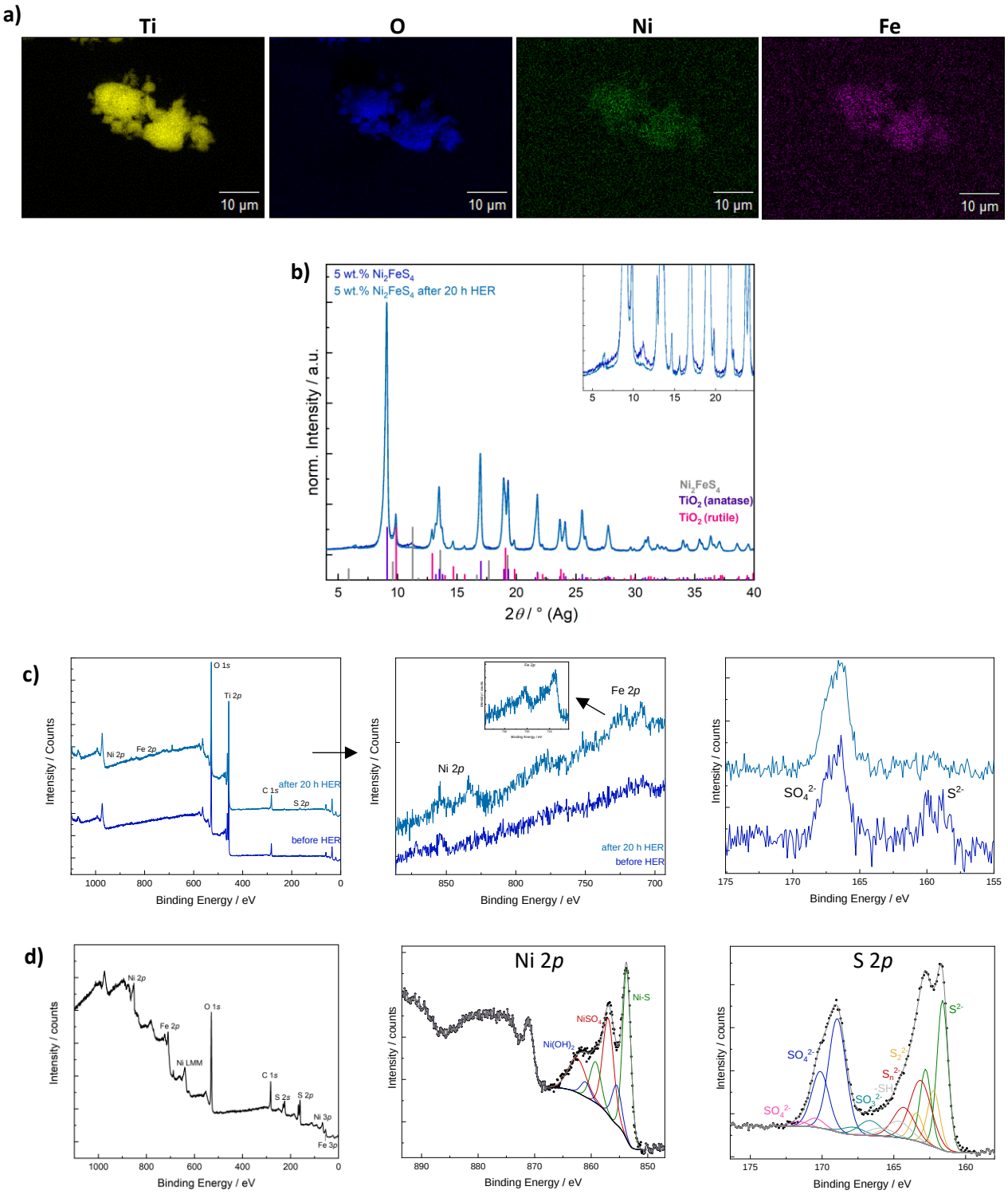

Figure S19 EDX mapping of 5 wt.% Ni_2FeS_4@P25 after irradiation for 20 h (a), Ag-XRD pattern for the same sample (b) and XPS results for 5 wt.% Ni_2FeS_4@P25 before and after the 20 h experiment(c), as well as for Ni_2FeS_4 stirred for 48 h in water.

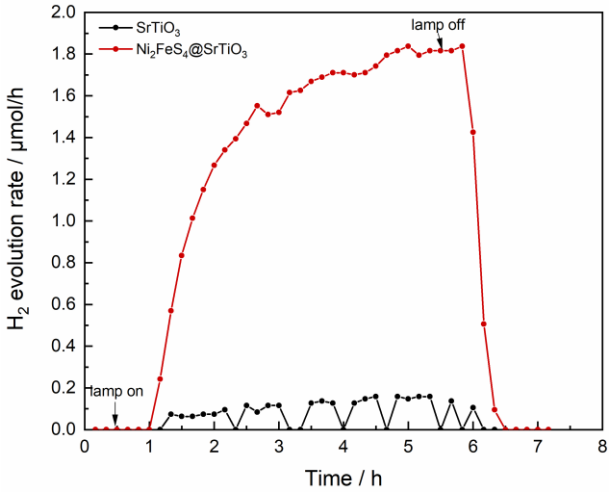

Figure S20 Hydrogen evolution over 5 wt.% of Ni_2FeS_4 on Al-doped $SrTiO_3$ under 1 sun simulated sunlight.